Forecasting ENSO with a Smooth Transition Autoregressive Model*

David Ubilava [a†] C. Gustav Helmers [b]

[a] Lecturer. Department of Agricultural and Resource Economics, The University of Sydney.
Add: R.D. Watt Building, Science Road, NSW 2006, Australia.
Tel: +61 (0)2 8627 1114; Fax: +61 (0)2 8627 1099; E-Mail: david.ubilava@sydney.edu.au
[b] Assistant Professor. Hutson School of Agriculture, Murray State University.

Add: 213 South Oakley Applied Science, Murray, KY 42071, USA.
Tel: +1 270 809 6932; Fax: +1 270 809 3441; E-mail: chelmers@murraystate.edu

Abstract

This study examines the benefits of nonlinear time series modelling to improve forecast accuracy of the El Niño Southern Oscillation (ENSO) phenomenon. The paper adopts a smooth transition autoregressive (STAR) modelling framework to assess the potentially smooth regime-dependent dynamics of the sea surface temperature anomaly. The results reveal STAR-type nonlinearities in ENSO dynamics, which results in the superior out-of-sample forecast performance of STAR over the linear autoregressive models. The advantage of nonlinear models is especially apparent in short- and intermediate-term forecasts. These results are of interest to researchers and policy makers in the fields of climate dynamics, agricultural production, and environmental management.

Keywords: El Niño Southern Oscillation; Out-of-Sample Forecasting; Smooth Transition Autoregression

*NOTICE: this is the authors' version of a work that was accepted for publication in Environmental Modelling & Software. Changes resulting from the publishing process, such as peer review, editing, corrections, structural formatting, and other quality control mechanisms may not be reflected in this document. Changes may have been made to this work since it was submitted for publication. A definitive version was subsequently published in Environmental Modelling & Software, Vol 40, Issue 1, (2013) doi: 10.1016/j.envsoft.2012.09.008

†Corresponding author

1 Introduction

Recent years have witnessed a growing interest in studying the role of weather anomalies on the performance of various economic variables (Keppenne, 1995; Brunner, 2002; Kim and McCarl, 2005). Researchers have paid particular attention to the large-scale medium-frequency event known as the El Niño Southern Oscillation (ENSO) (e.g. Glantz, 2001) and its economic effects (e.g. Handler, 1990; Carlson et al., 1996; Hansen et al., 1998; Legler et al., 1999). Studies have shown that the ENSO's impact on the world economy is significant. In the United States alone, some extreme episodes of ENSO have caused damages exceeding several billions of dollars (Adams et al., 1999; Pielke Jr and Landsea, 1999). Additionally, studies have found that ENSO's impact goes beyond its economic importance and affects social lives as well, to the extent that it may even cause civil conflicts in the developing world (Hsiang et al., 2011). The corollary is also true: society will benefit from the improved prediction of extreme ENSO events, as it will give economic agents and policy makers time to plan ahead. For example, the expected annual value of accurate ENSO prediction in the U.S. agricultural sector has been measured to be in the order of several hundred million dollars (Solow et al., 1998).

The aforementioned research indicates that ENSO could be a costly phenomenon and suggests that a better understanding and more accurate forecasts of this anomaly could potentially mitigate associated social and economic damages. Numerous data mining techniques have been implemented to improve the foundation of models relating to this phenomenon, such as using self organizing maps to reconstruct historical data (Friedel, 2012) or by connecting worldwide databases by Grid computing (Fernández-Quiruelas et al., 2011). In terms of the analysis, a variety of methods have been proposed and used to predict ENSO occurrences (e.g. Kirtman and Schopf, 1998; Halide and Ridd, 2008; Deng and Tang, 2009). Many of the implemented models are based on a linear relationship between the dependent variable and its autoregressive components (Chen and Cane, 2008). The International Research Institute for Climate and Society groups the ENSO forecast models into "dynamical" and "statistical" types, and Barnston et al. (2011) discusses a distinction between the groups. Of a particular interest to this research are statistical type models, which typically rely on analysis of historical time series data. For example, these statistical models include canonical correlations analysis by Barnston and Ropelewski (1992) and linear inverse modelling by Penland and Magorian (1993). Some models, such as ENSO-CLIPER by Knaff and Landsea (1997) for example, incorporate multivariate modelling techniques. Adding vectors of explanatory variables, i.e. multivariate modelling, is one way of improving ENSO forecast accuracy. An alternative approach to achieve the goal is to use nonlinear modelling techniques. This is particularly relevant as there is mounting evidence that ENSO cycles can be associated with nonlinear dynamics (e.g. Tang and Hsieh, 2002; An and Jin, 2004; Boucharel et al., 2011).

Recent developments in nonlinear time series modelling have allowed researchers to more thoroughly examine intricate dynamics of an ENSO cycle (e.g. Tangang et al., 1998;

Berliner et al., 2000; Hall et al., 2001; An, 2009). In this respect, climate literature has applied a modelling framework known as Artificial Neural Networks, or simply Neural Networks (NN), yielding considerable success in forecasting (e.g. Tangang et al., 1997; Tang and Hsieh, 2002). For an overview of this modelling framework, see Gardner and Dorling (1998), Fine (1999) and Teräsvirta et al. (2010). NNs are characterized by a flexibility to closely mimic nonlinearities associated with data. However, the flexibility comes at a cost in terms of computational complexities in the modelling stage, which is usually remedied by imposing a number of restrictions (see, for example, Teräsvirta et al., 2010).

In this research, we use an alternative nonlinear modelling approach to investigate regime-dependent asymmetries in ENSO dynamics – the smooth transition autoregressive (STAR) modelling framework of (Luukkonen et al., 1988) and (Teräsvirta, 1994). STAR models are considered "more parametrized" when compared to the "more nonparametric" NNs (Stock and Watson, 1998; Teräsvirta et al., 2005). Moreover, studies have shown that STAR models could potentially perform just as well and in some instances even outperform the NN models (e.g. Teräsvirta et al., 2005). This could also be true with respect to other statistical or dynamical models in the ENSO forecasting literature. Due to the STAR framework's inherent qualities, it is therefore possible that STAR would supplement the larger set of already well-established modelling techniques used in ENSO forecasting (see Barnston et al., 2011).

In the forecasting literature, STAR models have been advocated for their relative superiority in fitting turbulent variable dynamics (e.g. Teräsvirta, 1995). Thus, the STAR framework appears to be a suitable method to analyze potentially nonlinear ENSO dynamics, and has already been successfully applied by (Hall et al., 2001), who demonstrate support for distinct autocorrelations in ENSO anomalies in different El Niño and La Niña regimes. Based on these findings, Hall et al. (2001) suggest that point forecasts from nonlinear models are likely to outperform those from linear models. The primary focus of the current study is to examine whether the improvement in in-sample fit corresponds to a more accurate out-of-sample prediction of ENSO events.

The objective of this study is to assess ENSO forecast accuracy from STAR-type nonlinear models. We hypothesize that the parameters of nonlinear models facilitate improved forecast accuracy over their linear counterparts as well as simpler persistence measures. In what follows, we first present the methodological framework, describing the peculiarities of STAR modelling and forecasting. We then proceed by implementing this technique in the empirical framework. Using historical monthly Sea Surface Temperature (SST) data, we generate a sequence of out-of-sample forecasts from linear and nonlinear models, and examine them with respect to actual SST realizations. By means of statistical tests and graphical illustrations, we derive inferences about the forecast performance of linear and nonlinear models and, furthermore, relate these results to on-going studies in nonlinear time series and climatology literature.

2 Modelling Framework

The general idea behind time series modelling is that a current observation is a function of its previously observed values. Denote a variable of interest, i.e. the dependent variable, y_t, then a time series model in general terms can be expressed as in Equation (1):

$$y_t = g\left(x_t; \theta\right) + \varepsilon_t \tag{1}$$

where x_t is a vector containing autoregressive and, perhaps, exogenous variables; θ is a parameter vector; and ε_t is an additive error process such that $\varepsilon_t \sim iid(0, \sigma^2)$. A basic representation of this relationship is a linear autoregressive (AR) model, which may be expressed in a reparametrized form, suitable for the Augmented Dickey-Fuller (ADF) unit root testing framework (Dickey and Fuller, 1979), as in Equation (2):

$$\Delta y_t = \theta' x_t + \varepsilon_t \tag{2}$$

where Δ is a first-difference operator, such that $\Delta y_t = y_t - y_{t-1}$; $x_t = (1, y_{t-1}, \Delta y_{t-1}, \ldots, \Delta y_{t-p+1})'$ is a vector of right-hand-side variables; $\theta = (\alpha, \beta, \phi_1, \ldots, \phi_{p-1})'$ is a vector of autoregressive parameters, wherein β is the unit root parameter, such that the restriction $\beta = 0$ imposes a unit root process.

By relaxing the linearity assumption, Equation (2) can be further augmented in a number of ways, resulting in several well–known nonlinear time series frameworks such as threshold autoregressive (TAR) models (e.g. Tsay, 1989; Tong, 1990), Markov–switching models (e.g. Tyssedal and Tjøstheim, 1988; Hamilton, 1989), and Artificial Neural Networks (e.g. Kuan and White, 1994). An alternative specification, which is also a nonlinear generalization of a basic AR model, and moreover which embeds elements of the aforementioned nonlinear models, is the smooth transition autoregressive (STAR) model. Conceptually, smooth transition regressions were first proposed by Bacon and Watts (1971). Later, Chan and Tong (1986) suggested the use of the smooth transition framework in the time series setting. Subsequently, STAR modelling and testing methods were introduced and developed by Luukkonen et al. (1988), Teräsvirta and Anderson (1992), Teräsvirta (1994), and Eitrheim and Teräsvirta (1996).

STAR-type models have been widely applied in studies modelling asymmetric cyclical variations (e.g. Teräsvirta, 1995; Hall et al., 2001). One of the STAR modelling framework's attractive features is that it allows for non-discrete switching points between the extreme regimes, resulting in a potentially smooth transition between them (as noted in Teräsvirta et al. (2010), the lack of such smoothness has been a source of criticism for the TAR-type models, where the switch between regimes happens "instantaneously"). Since its introduction, the STAR modelling approach has gained popularity and has been increasingly applied in macroeconomic studies to examine the potential nonlinearities of unemployment rates, GDP, monetary demand, and interest rates (e.g. Teräsvirta, 1995; Eitrheim and Teräsvirta, 1996; Sarantis, 1999; Skalin and Teräsvirta, 2002). More recently, the

STAR modelling approach has been utilized to investigate nonlinear features of agricultural production and prices (e.g. Craig and Holt, 2008; Balagtas and Holt, 2009; Ubilava, 2012b), climate variables, including ENSO (Hall et al., 2001), and the effects of climate anomalies on commodity prices (Ubilava, 2012a).

The general class of smooth transition autoregressions can be specified as Equation (3):

$$\Delta y_t = \varphi_0{}' x_t + \varphi_1{}' x_t G\left(s_t; \gamma, c\right) + \varepsilon_t \tag{3}$$

where $G\left(s_t; \gamma, c\right)$ represents the so-called *transition function*, which is, by construction, bounded between zero and one, where s_t is a transition variable, and γ and c are, respectively, smoothness and location parameters. The transition function alters the dynamics of the model conditional on the transition variable in a potentially smooth manner.

A generalized version of one of the more frequently applied transition functions is represented as Equation (4):

$$G\left(s_t; \gamma, \mathbf{c}\right) = \left\{1 + \exp\left[-\gamma/\sigma_{s_t}^k \prod_k \left(s_t - c_k\right)^k\right]\right\}^{-1} \tag{4}$$

where σ_{s_t} is the standard deviation of the transition variable. By setting $k = 1$ and $k = 2$, one obtains *logistic* and *quadratic* transition functions, respectively, resulting in logistic STAR (LSTAR) and quadratic STAR (QSTAR) models. An alternative transition function is an *exponential* function, yielding an exponential STAR (ESTAR) model, and defined as Equation (5).

$$G\left(s_t; \gamma, c\right) = \left\{1 - \exp\left[-\gamma/\sigma_{s_t}^2 \left(s_t - c\right)^2\right]\right\} \tag{5}$$

In the transition functions, the smoothness parameter, γ, is defined to be a non-negative parameter. The LSTAR and QSTAR models converge to a linear AR model when $\gamma \to 0$, and a threshold autoregressive (TAR) model when $\gamma \to \infty$. Alternatively, ESTAR converges to a linear AR model both when either $\gamma \to 0$ or $\gamma \to \infty$.

2.1 Testing STAR-type Nonlinearities

The question of whether nonlinearity is truly an underlying feature of the data is a testable hypothesis. However, we cannot directly test the null hypothesis of linearity, that is, $H_0 : \gamma = 0$, in a STAR model due to unidentified nuisance parameters, also known as Davies' problem (Davies, 1977, 1987). Specifically, in the context of Equation (3), the nonlinear model will reduce to the linear AR model by imposing the restriction $\gamma = 0$ or $\theta_1 = 0$. Therefore, the standard test statistics are no longer applicable. Luukkonen et al. (1988) proposed a solution to the problem by approximating the transition function,

$G(s_t; \gamma, c)$, using a third order Taylor series expansion. This results in a testable auxiliary regression, expressed as Equation (6):

$$\Delta y_t = \theta_0{}' x_t + \sum_{i=1}^{3} \theta_i{}' x_t s_t^i + \xi_t \tag{6}$$

where ξ_t combines the original error term, ε_t, and the approximation error resulting from the Taylor expansion. The new specification allows the application of conventional testing methods, particularly in the test for linearity against the STAR specification. This is now equivalent to testing the null hypothesis of H_0': $\theta_1 = \theta_2 = \theta_3 = 0$, where θ_i, $i = 1, 2, 3$, are vectors of parameters from the auxiliary regression. An additional benefit of testing nonlinearities using a third order approximation, as presented in Equation (6), is that tests against LSTAR and ESTAR/QSTAR models are also embedded in the testing framework; the test against the LSTAR model is equivalent to testing the null hypotheses of H_{03}: $\theta_3 = 0$ and H_{01}: $\theta_1 = 0 | \theta_2 = \theta_3 = 0$. Alternatively, the test against the ESTAR/QSTAR is equivalent to H_{02}: $\theta_2 = 0 | \theta_3 = 0$.

In practice, the transition variable is often *a priori* unknown. One is, therefore, required to test a set of candidate transition variables and select the suitable transition variable based on probability values associated with the aforementioned hypotheses. Once the transition variable (and the associated transition function) is selected, one may proceed to estimate the related STAR model using a nonlinear optimization procedure (refer to Luukkonen et al. (1988); Teräsvirta (1995); Eitrheim and Teräsvirta (1996) for additional details regarding the testing procedure, including remaining nonlinearity, parameter constancy, and residual autocorrelation tests within the STAR modelling framework).

3 Out-of-Sample Forecasting and Forecast Evaluation

Consider a general specification of a univariate autoregression as in Equation (1). The expected one-step-ahead forecast can then be written as Equation (7).

$$y_{t+1|t} = g(y_t, \ldots, y_{t-p+1}) \tag{7}$$

Any h-step-ahead forecast, where $h > 1$, may be obtained recursively in a manner similar to Equation (7); however, in the case of nonlinear models, this so-called "naïve" or "skeleton extrapolation" approach would yield biased forecasts (see Tong, 1990; Granger and Teräsvirta, 1993). Alternatively, a proper, or so-called "exact" forecasting method, would require a numerical integration, which quickly becomes cumbersome as the forecast horizon length increases (e.g. Teräsvirta et al., 2010). This can be circumvented by approximating the multidimensional integral using a Monte-Carlo simulation or a bootstrap resampling method (e.g. Lundbergh and Teräsvirta, 2004). In this study, we will apply the bootstrapping technique, as it does not require knowledge of the exact distribution

of idiosyncratic shocks. Thus, for example, the expected two-step-ahead forecast can be written as Equation (8):

$$y_{t+2|t} = E\left\{y_{t+2}|\Re_t\right\} = E\left\{g\left(y_{t+1|t} + \varepsilon_{t+1}, y_t, \ldots, y_{t-p+2}\right)|\Re_t\right\} \tag{8}$$

where $\Re_t$ is the information set available at the time t. The bootstrap resampling method would then yield the expected value of $y_{t+2|t}$:

$$y^b_{t+2|t} = B^{-1}\sum_{b=1}^{B} g\left(y_{t+1|t} + \hat{\varepsilon}^b_{t+1}, y_t, \ldots, y_{t-p+2}\right) \tag{9}$$

where $\hat{\varepsilon}^b_{t+1}$ is the bth independent draw with replacement from the set of residuals of the estimated model, $\hat{\varepsilon}_1, \ldots, \hat{\varepsilon}_T$. An h-step-ahead forecast can thus be developed in a manner similar to Equations (8) and (9). Finally, by applying the bootstrap resampling method, one can effectively generate a distribution of forecasts around the mean. Therefore, this approach can also be useful if one intends to calculate the forecasts' empirical confidence intervals, including in the linear models.

3.1 Out-of-Sample Forecast Evaluation

Out-of-sample forecasts are evaluated using forecast accuracy measures, the most frequently applied one being root mean squared (forecast) errors (RMSE), defined as Equation (10):

$$\hat{\sigma}_{b,t+h|t} = \left[R^{-1}\sum_{r=1}^{R}\left(y_{r,t+h} - y^b_{r,t+h|t}\right)^2\right]^{\frac{1}{2}} \tag{10}$$

where $y_{r,t+h}$ is the actual realization of the event at the horizon h; $y^b_{r,t+h|t}$ is the event forecast for the horizon h; and R is the total number of out-of-sample forecasts.

The smaller is the RMSE measure, the better is a particular forecast. So, in order to compare the forecast "skills" of two competing models, one should assess a relative difference between two RMSE measures. A number of methods have been proposed to assess forecast accuracies. One of the most frequently applied methods is a Diebold-Mariano (DM) measure (proposed by Diebold and Mariano (1995) and later augmented by Harvey et al. (1997)). However, when one of the competing models nests another (which is the case in the current research), then the DM measure is not applicable (e.g. Clark and McCracken, 2001). For such cases, alternative measures have been proposed in lieu of the DM measure. In this study, we will use one such measure proposed by Clark and West (2007) (subsequently referred to as CW). Consider forecast errors from two competing models: $e^l_{r,t+h|t} = \left(y_{r,t+h} - y^l_{r,t+h|t}\right)$ and $e^n_{r,t+h|t} = \left(y_{r,t+h} - y^n_{r,t+h|t}\right)$, where $y^n_{r,t+h|t}$ and $y^l_{r,t+h|t}$ are h-step-ahead forecasts from, say, the nonlinear and linear models,

such that the nonlinear model nests the linear counterpart. Further, define an "adjustment error" as follows: $e^a_{r,t+h|t} = \left(y^l_{r,t+h|t} - y^n_{r,t+h|t}\right)$. Then, the null hypothesis of equal mean squared (forecast) errors is rejected if the difference given by $\hat{\sigma}^2_{l,t+h|t} - (\hat{\sigma}^2_{n,t+h|t} - \hat{\sigma}^2_{a,t+h|t})$ is sufficiently positive (for more details see Clark and West, 2007); here $\hat{\sigma}^2_{l,t+h|t}$, $\hat{\sigma}^2_{n,t+h|t}$ and $\hat{\sigma}^2_{a,t+h|t}$ are obtained in a way consistent with Equation (10).

4 Empirical Framework

In this section, we apply the methodology outlined in the previous section to obtain estimates for the linear and nonlinear models. These estimates are then used to forecast ENSO and perform an out-of-sample forecast accuracy test.

4.1 Data

The sample consists of monthly observations between January 1950 and December 2011. The time series variable representing the ENSO anomaly, *Niño 3.4*, is derived from the index tabulated by the Climate Prediction Center at the National Oceanic and Atmospheric Administration. This index measures the difference in Sea Surface Temperature (SST) in the area of the Pacific Ocean between $5°N - 5°S$ and $170°W - 120°W$, and is therefore a strong indicator of ENSO's occurrence in the tropical Pacific. The *Niño 3.4* monthly measure is an average of daily values interpolated from weekly measures obtained from both satellites and actual locations around the Pacific. The SST anomaly is the deviation of the *Niño 3.4* monthly measure from the average historic measure for that particular month from the period 1971 – 2000.

The econometric model, as well as simulations, utilize the monthly data. However, for the purposes of presentation, we create 3-month running means so that the results of this study are consistent and comparable with other studies in the climatology literature (see, for example, Barnston et al., 2011). Figure 1 presents the 3-month running means of the *Niño 3.4* index (panel (a)), where El Niño and La Niña occurrences are highlighted (defined as 3-month running mean being above $0.45°C$ and below -0.45°C, respectively). Panel (b) of Figure 1 features one-year-ahead ENSO dynamics, following El Niño and La Niña conditions during the NDJ (November-December-January) period. The graph indicates the potentially asymmetric nature of ENSO cycles, wherein El Niño episodes tend to be followed by La Niña, but the opposite is usually not the case. This further justifies the importance of nonlinear time series modelling of ENSO dynamics.

In order to generate out-of-sample forecasts, we employ an expanding window modelling approach (e.g. Teräsvirta et al., 2005). The benefit of this approach, as opposed to a fixed-length rolling window approach (e.g. Milas and Rothman, 2008), is that at any point of time we employ the maximum historical information available. On the other hand, the potential drawback of this approach is the de-emphasized possibility of structural breaks

(see Swanson, 1998; Teräsvirta et al., 2005). However, we took advantage of parameter constancy tests in the STAR testing framework to ascertain that there is indeed no evidence of a structural change in any of the windows employed. Therefore, we proceeded by estimating STAR models using an expanding window framework. We simulate a set of h-step-ahead forecasts for each window, where the maximum horizon length, h_{max}, is set to 36 months. The first estimation window covers the period from January 1952 to December 1990, and the last window ends with December 2008. Within this range, each consecutive window is estimated by expanding the window ahead by one observation, which in our case constitutes one month. This approach generates a total of 216 h-step-ahead forecasts, $h = 1, \ldots, h_{max}$. Finally, similar to Teräsvirta et al. (2005), while the models are re-estimated on a monthly basis, the autoregressive lag structure and the delay lag of the transition variable are re-examined on an annual basis.

4.2 Estimation Results

We use the ADF test to examine the stationarity hypothesis of the ENSO variable. Based on the test results, we reject the unit root hypotheses in the ENSO series in each expanding window, meaning that despite shocks of any magnitude, over time the ENSO anomaly returns to its long-run mean. Thus, the following linear version of the regression as in Equation (11) was estimated:

$$\Delta \text{ENSO}_t = \alpha + \beta \text{ENSO}_{t-1} + \sum_{i=1}^{p-1} \theta_i \Delta \text{ENSO}_{t-i} + \delta' \text{D}_t + \varepsilon_t \tag{11}$$

where ENSO_t denotes the SST anomaly used in this research, D_t is a vector of monthly dummy variables; p is the optimal lag length as selected based on the Schwarz criterion (SC, Schwarz, 1978) and the Breusch-Godfrey residual autocorrelation test results (Breusch, 1978; Godfrey, 1978); further, $\varepsilon_t \sim iid(0, \sigma^2)$, and the rest are parameters to be estimated.

Next, we assess STAR-type nonlinearities in each of the windows. We use the lags of the ENSO variable, ENSO_{t-d}, $d = 1, \ldots, 6$, as candidate transition variables. Thus, we allow for the possibility that ENSO dynamics will vary conditionally on its recent past occurrence. For example, depending on the recent conditions of the anomaly, ENSO's adjustment to its long-run mean may happen at a different speed. It should be noted that the nonlinearities are assessed for the equation's autoregressive components as well as the seasonal dummy variables. There is climatological support for the idea of conditioning ENSO seasonal effects on ENSO occurrences. For example, depending on previously observed ENSO conditions, a certain month's SST anomaly could vary (e.g. Knaff and Landsea, 1997). Moreover, we also found statistical evidence (based on Teräsvirta's (1994) test performed solely on seasonal dummy variables), suggesting nonlinearities in seasonal parameters with respect to lagged ENSO variables.

A battery of nonlinearity and other diagnostic test results reveal evidence of two-regime STAR-type nonlinearities throughout all considered windows (see Table 1; for the sake

of brevity, here we only present the nonlinearity test results for one expanding window. Results for all other windows are available upon request). The test results reveal apparent logistic type nonlinearities. Moreover, after estimating the two-regime STAR model, there is very little evidence of remaining nonlinearities. Notably, in all other estimated windows, the nonlinearities appear to be of a logistic form as well, which constitutes the criterion for choosing the LSTAR model specification in every considered expanding window. Thus, we formulate our final specification as in Equation (12):

$$\begin{aligned} \Delta \text{ENSO}_t &= \alpha_0 + \beta_0 \text{ENSO}_{t-1} + \sum_{i=1}^{p-1} \theta_{0,i} \Delta \text{ENSO}_{t-i} + \delta_0' \text{D}_t \\ &+ \left(\alpha_1 + \beta_1 \text{ENSO}_{t-1} + \sum_{i=1}^{p-1} \theta_{1,i} \Delta \text{ENSO}_{t-i} + \delta_1' \text{D}_t \right) G(\cdot) + \varepsilon_t \end{aligned} \tag{12}$$

where the transition function, $G(\cdot)$, is defined as Equation (13).

$$G(\cdot) = \{1 + \exp[-\gamma/\sigma (\text{ENSO}_{t-d} - c)]\}^{-1} \tag{13}$$

The estimated parameters of the transition function suggest a smooth transition between the extreme regimes. To illustrate ENSO dynamics, we present the estimated parameters of linear AR and nonlinear STAR models for the period between January 1952 and December 2007 (see Table 2). Additionally, we present the estimated parameters of the transition function in Equation (14).

$$G(s_t; \hat{\gamma}, \hat{c}) = \left\{ 1 + \exp\left[\underset{(0.514)}{-1.196} / 0.835 \left(ENSO_{t-1} + \underset{(0.463)}{0.447} \right) \right] \right\}^{-1} \tag{14}$$

The low value of the γ parameter suggests a smooth (continuous) curvature of the associated transition function. For a better representation, the estimated transition function and the associated transition variable are illustrated in Figure 3. The figure indicates a smooth transition between the extreme regimes. Note that the inflection point, $G = 0.5$, of the transition function is slightly below zero ($\hat{c} = -0.447$), however, because of the smoothness of the transition function, we observe a continuum of inflection points, such that the normal ENSO regime can be characterized by the dynamics which is a weighted average of the dynamics underlying the two extreme regimes. In other words, at any given period of time, a set of parameters underlying the dynamics, $\phi_{w,t}$, will be a weighted average of the $\phi_{0,t} = \varphi_{0,t}$ and $\phi_{1,t} = \varphi_{0,t} + \varphi_{1,t}$ parameters of each of the extreme regimes, where weights are $\{1 - G(s_t; \gamma, c)\}$ and $\{G(s_t; \gamma, c)\}$, respectively, based on a realization of the transition function in that period.

The estimated parameters, $\varphi_{0,t}$ and $\varphi_{1,t}$, associated with these two extreme regimes are presented in Table 2. Along with the parameters from the STAR model, the table also presents estimated parameters, θ, from the linear AR model for comparison purposes. For

example, consider unit root parameters: both linear and nonlinear models suggest a mean-reverting process (unit root parameters are statistically significantly different from zero). However, based on STAR estimates we observe an increase (in absolute terms) of the unit root parameter when moving from a La Niña regime ($G(s_t;\gamma,c) \to 0$) to an El Niño regime ($G(s_t;\gamma,c) \to 1$). This well-reflects the ENSO cycle's observed patterns in that El Niño phases typically last for shorter periods, often followed by La Niña phases, which usually last for more extended periods, often gradually returning to neutral conditions (refer also to Figure 1).

4.3 Forecasting

We use the estimated parameters and residuals from the linear and nonlinear models from each expanding window to calculate out-of-sample forecasts. We obtain ENSO forecasts using a bootstrap resampling approach. Specifically, we simulate B paths of $E_{t+1|t}, E_{t+2|t}, \ldots, E_{t+h_{max}|t}$, where $B = 1000$ is the total amount of paths, and $h_{max} = 36$ is the maximum horizon length. So, for a given path b, the h-step-ahead forecast of ENSO is formulated as Equation (15):

$$\text{ENSO}^b_{t+h|t} = f\left(\text{ENSO}^b_{t+h-1|t}, \ldots, ENSO^b_{t+h-p|t} | \Re\right) + \varepsilon^b_{t+h|t} \tag{15}$$

where p is the autoregressive lag length of the ENSO variable, and where $ENSO^b_{t+h-p|t} = ENSO_{t+h-p|t}$ if $p \geq h$; $\varepsilon^b_{t+h|t}$ is an innovation sampled from the pool of residuals of the estimated ENSO model. We implement a block-bootstrap approach to mitigate the effects of potential residual autocorrelation and heteroskedasticity. Based on these monthly forecasts, we also calculate the three-month-average measures of the SST anomaly. Further, we obtain expected forecasts by averaging the computed bootstrap paths. These forecasts are subsequently used to evaluate the forecast accuracy of linear and nonlinear models using the RMSE measures and the associated test statistics, as previously defined.

We evaluate the forecasts from AR and STAR models in relation to the actual realizations of ENSO. Additionally, we calculate persistence measures of ENSO, wherein "persistence" is defined as $ENSO^p_{t+h|t} = ENSO_t$, and thus represents a "no change forecast" (e.g. Stock and Watson, 1998). The ultimate goal is to assess the ENSO forecast accuracy improvement from more sophisticated models over the "more simple" ones. That is, we compare the STAR and AR model performance to the persistence benchmark, and, also, the STAR model performance to the linear alternative.

We first illustrate the relative forecast ability of AR and STAR models, along with the persistence benchmark, by evaluating correlations up to a 12-month-ahead period. Moreover, we obtain these correlation measures from each of the 12 three-month-periods as a starting point. These correlations are presented in Figure 2. Additionally, the correlation figures feature the threshold contours of 0.9, 0.7 and 0.5, and correlations exceeding each of those thresholds, respectively, represent "good," "satisfactory" and "usable" forecasts as

defined by Barnston and Ropelewski (1992). First, note the presence of the so-called "spring barrier" – in all three cases, the forecasts made right before or during the MAM (average of March–April–May SST anomalies) season are inferior to those made after the JAS (July–August–September) season. Even so, we observe apparent superiority of forecasts from the STAR model to those based on either the AR model or persistence.

We further illustrate the potential advantage of the STAR modelling framework by assessing the ability to forecast extreme events. Our definition of ENSO events are comparable to those used by The International Research Institute for Climate and Society, in that we define La Niña as when the three-month running mean of the SST anomaly goes below $-0.45°C$, and El Niño as when the three-month running mean of the SST anomaly exceeds $0.45°C$. Additionally, for illustration purposes, we introduce notions of "extreme" events, wherein the thresholds are $-0.9°C$ and $0.9°C$, respectively. In recent history, the 1997-1998 period was an interesting one because it featured one of the strongest El Niño events in the past several decades, which was then followed by a strong La Niña. We use empirical forecast densities from the previously discussed bootstrap resampling procedure to compile probability forecasts of ENSO events from the STAR and AR models. We illustrate predicted probabilities of ENSO events in Figures 4 and 5. In Figure 4, the forecasts are made using information up to and including the AMJ (April–May–June) season of 1997 – when ENSO conditions were near-neutral. As seen, the STAR model predicted the upcoming El Niño (one of the most extreme El Niño occurrence in recent history) with far better accuracy than the AR model. Figure 5, on the other hand, features forecasts made during the peak of the mentioned El Niño event. Again, even though in the short run (1–3 months) linear and nonlinear models yield comparable results, the picture changes in the intermediate run (6–12 months), when the STAR model predicts the La Niña episode with about 70 percent probability, while the AR model predicts the La Niña with a "modest" 30 percent probability. In reality, the 1997 El Niño was indeed followed by a strong La Niña in late 1998, which carried over into 1999 and 2000. This illustration is characteristic of the STAR model in that it is especially effective in predicting extreme ENSO occurrences in the intermediate run.

The preceding discussion indicated the clear advantages of nonlinear modelling. We will now assess the statistical significance of these superiorities. We do so by obtaining the RMSE measures (as defined in Equation (10)), and examine forecast accuracy improvement using the CW (Clark and West, 2007) approach. The results of this analysis are presented in Table 3. First, the results indicate statistically significant improvements of ENSO forecast ability by both AR and STAR models relative to a simple persistence measure. More interestingly, the results confirm that not only does the STAR specification improve the in-sample fit, but it also outperforms the corresponding AR model in an out-of-sample setting. This improvement is apparent (statistically significant) for an up to one-and-a-half year ahead forecast horizon.

Finally, we use point forecasts of the SST anomalies to calculate percent correctly predicted (PCP) measures of ENSO events. To do so, we define El Niño and La Niña

events as an SST anomaly being greater than $0.45°C$ and less than -$0.45°C$, respectively. Columns 7 – 10 of Table 3 present the PCP measures from AR and STAR models. Here as well, the relative advantage of nonlinear modelling becomes apparent at and beyond 3-months-ahead forecast horizons. This reveals two features of interest. First, the forecast horizon for ENSO events are notably longer using the STAR as compared to AR models. Second, models predict La Niña events more accurately than El Niño events.

5 Conclusions

ENSO is a costly phenomenon, causing considerable economic damages around the globe (Handler, 1990; Solow et al., 1998; Brunner, 2002). It has also been considered a factor in social unrest and even civil wars (Hsiang et al., 2011). Given the important nature of this climatic anomaly, researchers have attempted to improve its predictability with some success. One way to improve the forecast accuracy of ENSO that has been proposed is to implement recent developments in nonlinear time series modelling, and specifically the smooth transition autoregressive framework of Luukkonen et al. (1988) and Teräsvirta and Anderson (1992). Using the same methodology, Hall et al. (2001) have found that ENSO does follow a regime-dependent dynamic process, wherein the regimes are connected to each other in a smooth manner. As noted by Hall et al. (2001) the STAR framework offers an improved in-sample fit, suggesting the possibility of an improved out-of-sample fit as well.

In this research, we extended the study by Hall et al. (2001) to investigate out-of-sample predicting accuracy of the ENSO phenomenon. We found that forecasts from the nonlinear STAR model indeed outperform their counterparts from the linear AR model in the short and intermediate terms, while both models outperform the simple benchmark of persistence at every considered forecast horizon (up to three years ahead). These results are important for economic agents and policy makers world-wide, as they offer improved ENSO forecasting and more accurate economic and social inferences. The results are also interesting from a nonlinear time series research standpoint, wherein this study is an addition to a series of studies suggesting the preference of nonlinear models in ENSO forecasting. Finally, this study establishes a platform for future research in a number of different ways. The most interesting of which, both from the nonlinear time series modelling and the climate forecasting standpoint, is the potential to implement a multivariate version of the current smooth transition framework, known as smooth transition vector autoregression, and further improve ENSO forecast accuracy by incorporating Southern Oscillation Index (SOI) and SST indices from other *Niño* regions.

References

Adams, R., C. Chen, B. McCarl, and R. Weiher (1999). The Economic Consequences of ENSO Events for Agriculture. *Climate Research 13*(3), 165–172.

An, S. (2009). A Review of Interdecadal Changes in the Nonlinearity of the El Nino - Southern Oscillation. *Theoretical and Applied Climatology 97*(1), 29–40.

An, S. and F. Jin (2004). Nonlinearity and Asymmetry of ENSO. *Journal of Climate 17*(12), 2399–2412.

Bacon, D. and D. Watts (1971). Estimating the Transition between Two Intersecting Straight Lines. *Biometrika 58*(3), 525.

Balagtas, J. and M. Holt (2009). The Commodity Terms of Trade, Unit Roots, and Nonlinear Alternatives: A Smooth Transition Approach. *American Journal of Agricultural Economics 91*(1), 87–105.

Barnston, A. and C. Ropelewski (1992). Prediction of ENSO Episodes using Canonical Correlation Analysis. *Journal of climate 5*(11), 1316–1345.

Barnston, A., M. Tippett, M. LHeureux, S. Li, and D. Dewitt (2011). Skill of Real-time Seasonal ENSO Model Predictions during 2002-2011 – Is Our Capability Increasing? *Bulletin of the American Meteorological Society*. doi: 10.1175/BAMS-D-11-00111.1.

Berliner, L., C. Wikle, and N. Cressie (2000). Long-Lead Prediction of Pacific SSTs via Bayesian Dynamic Modeling. *Journal of Climate 13*(22), 3953–3968.

Boucharel, J., B. Dewitte, Y. du Penhoat, B. Garel, S. Yeh, and J. Kug (2011). ENSO Nonlinearity in a Warming Climate. *Climate Dynamics 37*, 2045–2065.

Breusch, T. (1978). Testing for Autocorrelation in Dynamic Linear Models. *Australian Economic Papers 17*(31), 334–55.

Brunner, A. (2002). El Nino and World Primary Commodity Prices: Warm Water or Hot Air? *Review of Economics and Statistics 84*(1), 176–183.

Carlson, R., D. Todey, and S. Taylor (1996). Midwestern Corn Yield and Weather in Relation to Extremes of the Southern Oscillation. *Journal of Production Agriculture 9*(3), 347–352.

Chan, K. and H. Tong (1986). On Estimating Thresholds in Autoregressive Models. *Journal of time series analysis 7*(3), 179–190.

Chen, D. and M. Cane (2008). El Niño Prediction and Predictability. *Journal of Computational Physics 227*(7), 3625–3640.

Clark, T. and M. McCracken (2001). Tests of Equal Forecast Accuracy and Encompassing for Nested Models. *Journal of Econometrics 105*(1), 85–110.

Clark, T. and K. West (2007). Approximately Normal Tests for Equal Predictive Accuracy in Nested Models. *Journal of Econometrics 138*(1), 291–311.

Craig, L. A. and M. T. Holt (2008, January). Mechanical Refrigeration, Seasonality, and the Hog-Corn Cycle in the United States: 1870-1940. *Explorations in Economic History 45*(1), 30–50.

Davies, R. (1977). Hypothesis Testing when a Nuisance Parameter is Present only under the Alternative. *Biometrika 64*(2), 247–254.

Davies, R. (1987). Hypothesis Testing when a Nuisance Parameter is Present only under the Alternative. *Biometrika 74*(1), 33–43.

Deng, Z. and Y. Tang (2009). The Retrospective Prediction of ENSO from 1881 to 2000 by a Hybrid Coupled Model: (II) Interdecadal and Decadal Variations in Predictability. *Climate Dynamics 32*(2), 415–428.

Dickey, D. and W. Fuller (1979). Distribution of the Estimators for Autoregressive Time Series with a Unit Root. *Journal of the American statistical association 74*(366), 427–431.

Diebold, F. and R. Mariano (1995). Comparing Predictive Accuracy. *Journal of Business & Economic Statistics 13*(3), 253–263.

Eitrheim, O. and T. Teräsvirta (1996). Testing the Adequacy of Smooth Transition Autoregressive Models. *Journal of Econometrics 74*(1), 59–75.

Fernández-Quiruelas, V., J. Fernández, A. Cofiņo, L. Fita, and J. Gutiérrez (2011). Benefits and Requirements of Grid Computing for Climate Applications. An Example with the Community Atmospheric Model. *Environmental Modelling & Software*.

Fine, T. (1999). *Feedforward Neural Network Methodology*. Springer Verlag.

Friedel, M. (2012). Data-Driven Modeling of Surface Temperature Anomaly and Solar Activity Trends. *Environmental Modelling & Software*.

Gardner, M. and S. Dorling (1998). Artificial Neural Networks (the multilayer perceptron) – a Review of Applications in the Atmospheric Sciences. *Atmospheric environment 32*(14-15), 2627–2636.

Glantz, M. (2001). *Currents of Change: Impacts of El Niño and La Niña on Climate and Society*. Cambridge Univ Pr.

Godfrey, L. (1978). Testing against General Autoregressive and Moving Average Error Models When the Regressors Include Lagged Dependent Variables. *Econometrica 46*(6), 1293–1301.

Granger, C. and T. Teräsvirta (1993). *Modelling Nonlinear Economic Relationships*. Oxford University Press, USA.

Halide, H. and P. Ridd (2008). Complicated ENSO Models Do Not Significantly Outperform Very Simple ENSO Models. *International Journal of Climatology 28*(2), 219–233.

Hall, A., J. Skalin, and T. Teräsvirta (2001). A Nonlinear Time Series Model of El Niño. *Environmental Modelling and Software 16*(2), 139–146.

Hamilton, J. D. (1989). A New Approach to the Economic Analysis of Nonstationary Time Series and the Business Cycle. *Econometrica 57*(2), 357–384.

Handler, P. (1990). USA Corn Yields, The El Niño and Agricultural Drought: 1867–1988. *International Journal of Climatology 10*(8), 819–828.

Hansen, J., A. Hodges, and J. Jones (1998). ENSO Influences on Agriculture in the Southeastern United States. *Journal of Climate 11*(3), 404–411.

Harvey, D., S. Leybourne, and P. Newbold (1997). Testing the Equality of Prediction Mean Squared Errors. *International Journal of Forecasting 13*(2), 281–291.

Hsiang, S., K. Meng, and M. Cane (2011). Civil Conflicts are Associated with the Global Climate. *Nature 476*, 438–441.

Jarque, C. and A. Bera (1987). A test for Normality of Observations and Regression Residuals. *International Statistical Review 55*(2), 163–172.

Keppenne, C. (1995). An ENSO Signal in Soybean Futures Prices. *Journal of Climate 8*(6), 1685–1689.

Kim, M. and B. McCarl (2005). The Agricultural Value of Information on the North Atlantic Oscillation: Yield and Economic Effects. *Climatic Change 71*(1), 117–139.

Kirtman, B. and P. Schopf (1998). Decadal Variability in ENSO Predictability and Prediction. *Journal of Climate 11*(11), 2804–2822.

Knaff, J. and C. Landsea (1997). An El Nino–Southern Oscillation Climatology and Persistence (CLIPER) Forecasting Scheme. *Weather and Forecasting 12*(3), 633–652.

Kuan, C.-M. and H. White (1994). Artificial Neural Networks: An Econometric Perspective. *Econometric Reviews 13*(1), 1–91.

Legler, D., K. Bryant, and J. O'Brien (1999). Impact of ENSO-related Climate Anomalies on Crop Yields in the U.S. *Climatic Change 42*(2), 351–375.

Lomnicki, Z. (1961). Tests for Departure from Normality in the Case of Linear Stochastic Processes. *Metrika 4*(1), 37–62.

Lundbergh, S. and T. Teräsvirta (2004). Forecasting with Smooth Transition Autoregressive Models. In M. P. Clements and D. F. Hendry (Eds.), *A Companion to Economic Forecasting*, pp. 485–509. Blackwell Publishing.

Luukkonen, R., P. Saikkonen, and T. Teräsvirta (1988). Testing Linearity Against Smooth Transition Autoregressive Models. *Biometrika 75*(3), 491–499.

Milas, C. and P. Rothman (2008). Out-of-Sample Forecasting of Unemployment Rates with Pooled STVECM Forecasts. *International Journal of Forecasting 24*(1), 101–121.

Penland, C. and T. Magorian (1993). Prediction of Niño 3 Sea Surface Temperatures using Linear Inverse Modeling. *Journal of Climate 6*(6), 1067–1076.

Pielke Jr, R. and C. Landsea (1999). La Nina, El Nino, and Atlantic Hurricane Damages in the United States. *Bulletin of the American Meteorological Society 80*(10), 2027–2034.

Sarantis, N. (1999). Modeling Non-linearities in Real Effective Exchange Rates. *Journal of International Money and Finance 18*(1), 27–45.

Schwarz, G. (1978). Estimating the Dimension of a Model. *The Annals of Statistics 6*(2), 461–464.

Skalin, J. and T. Teräsvirta (2002). Modeling Asymmetries and Moving Equilibria in Unemployment Rates. *Macroeconomic Dynamics 6*(2), 202–241.

Solow, A., R. Adams, K. Bryant, D. Legler, J. O'Brien, B. McCarl, W. Nayda, and R. Weiher (1998). The Value of Improved ENSO Prediction to US Agriculture. *Climatic Change 39*(1), 47–60.

Stock, J. H. and M. W. Watson (1998, June). A Comparison of Linear and Nonlinear Univariate Models for Forecasting Macroeconomic Time Series. NBER Working Papers 6607, National Bureau of Economic Research, Inc.

Swanson, N. (1998). Money and Output Viewed through a Rolling Window. *Journal of Monetary Economics 41*(3), 455–473.

Tang, Y. and W. Hsieh (2002). Hybrid Coupled Models of the Tropical Pacific: II ENSO prediction. *Climate dynamics 19*(3), 343–353.

Tangang, F., W. Hsieh, and B. Tang (1997). Forecasting the Equatorial Pacific Sea Surface Temperatures by Neural Network Models. *Climate Dynamics 13*(2), 135–147.

Tangang, F., B. Tang, A. Monahan, and W. Hsieh (1998). Forecasting ENSO Events: A Neural Network – Extended EOF Approach. *Journal of Climate 11*(1), 29–41.

Teräsvirta, T. (1994). Specification, Estimation, and Evaluation of Smooth Transition Autoregressive Models. *Journal of the American Statistical Association 89*(425), 208–218.

Teräsvirta, T. (1995). Modelling Nonlinearity in US Gross National Product 1889–1987. *Empirical Economics 20*(4), 577–597.

Teräsvirta, T. and H. Anderson (1992). Characterizing Nonlinearities in Business Cycles using Smooth Transition Autoregressive Models. *Journal of Applied Econometrics 7*, S119–S136.

Teräsvirta, T., D. Tjøstheim, and C. W. J. Granger (2010, December). *Modelling Nonlinear Economic Time Series*. Number 9780199587155 in OUP Catalogue. Oxford University Press.

Teräsvirta, T., D. Van Dijk, and M. Medeiros (2005). Linear Models, Smooth Transition Autoregressions, and Neural Networks for Forecasting Macroeconomic Time Series: A Re-examination. *International Journal of Forecasting 21*(4), 755–774.

Tong, H. (1990). *Non-linear Time Series: A Dynamical System Approach*. Oxford University Press.

Tsay, R. (1989). Testing and Modeling Threshold Autoregressive Processes. *Journal of the American Statistical Association 84*(405), 231–240.

Tyssedal, J. and D. Tjøstheim (1988). An Autoregressive Model with Suddenly Changing Parameters and an Application to Stock Market Prices. *Applied statistics 37*(3), 353–369.

Ubilava, D. (2012a). El Niño, La Niña, and World Coffee Price Dynamics. *Agricultural Economics 43*(1), 17–26.

Ubilava, D. (2012b). Modeling Nonlinearities in the U.S. Soybean-to-Corn Price Ratio: A Smooth Transition Autoregression Approach. *Agribusiness: an International Journal 28*(1), 29–41.

6 Figures

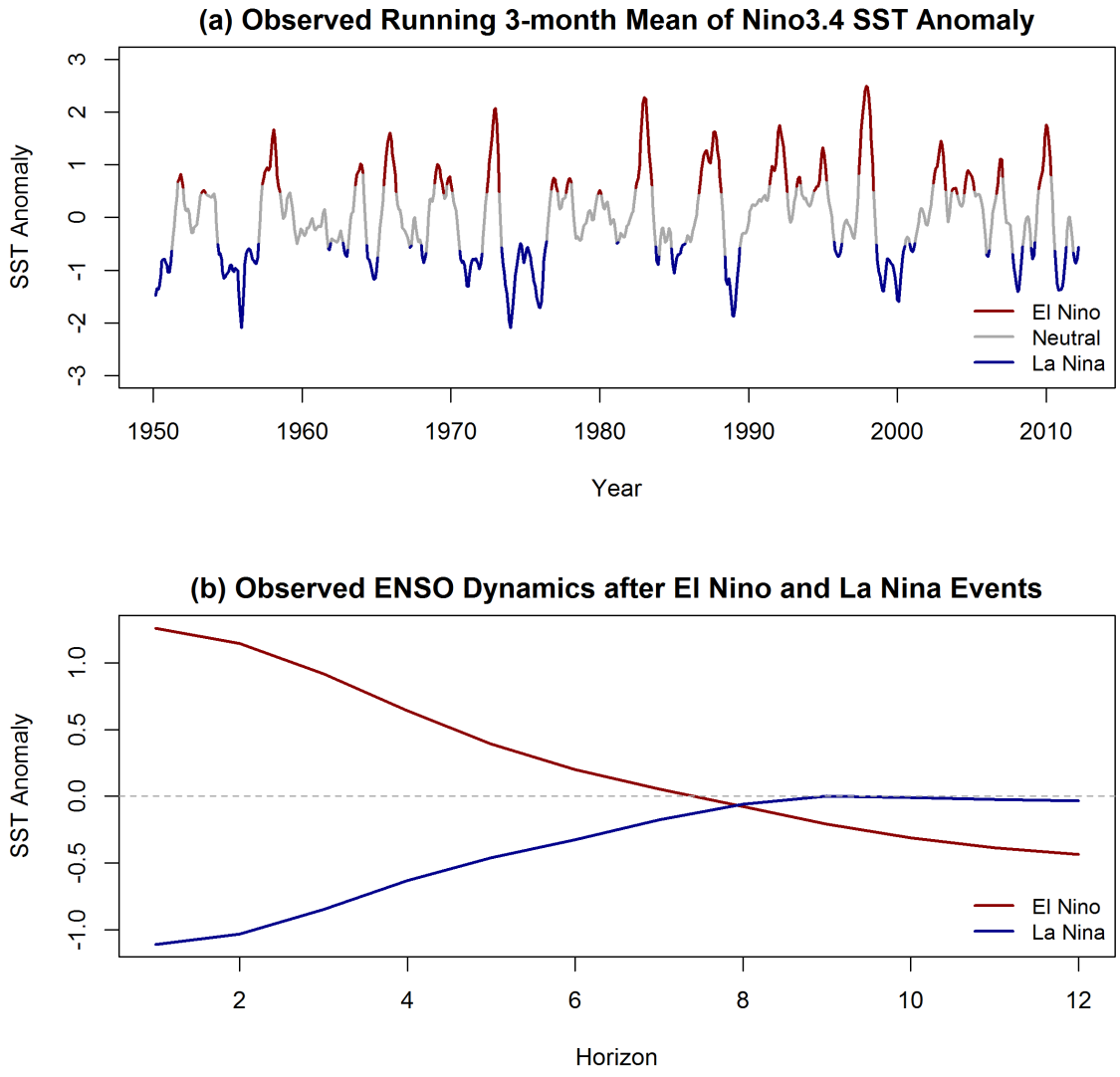

Figure 1: Historical ENSO Dynamics

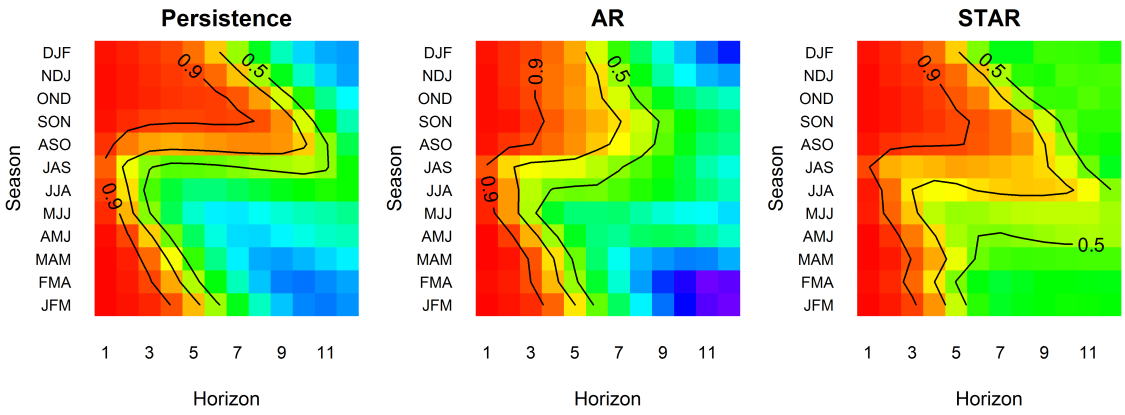

Figure 2: Correlations between Actual and Predicted SST Anomaly Measures

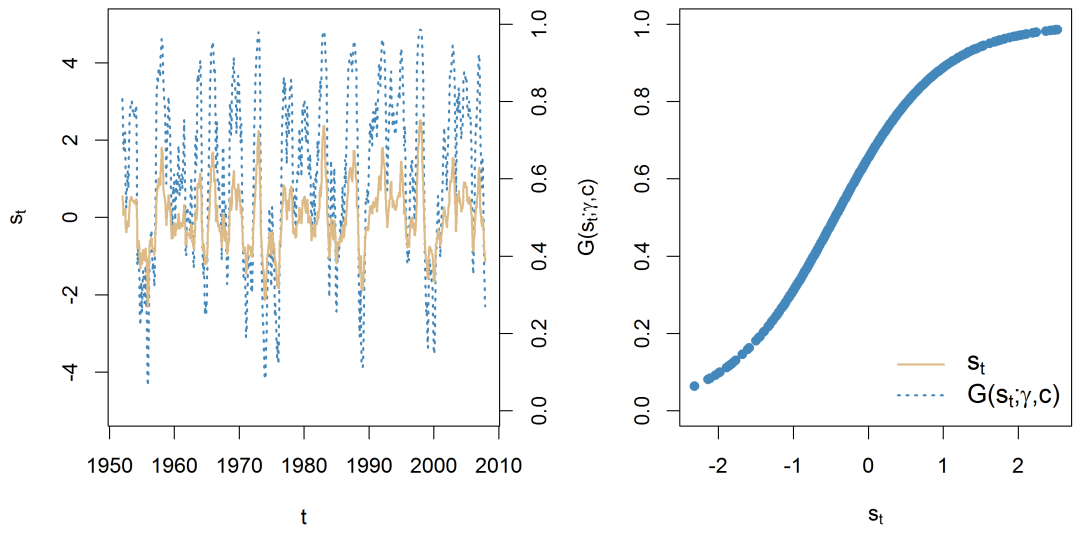

Figure 3: Estimated Transition Function (January 1952 – December 2007)

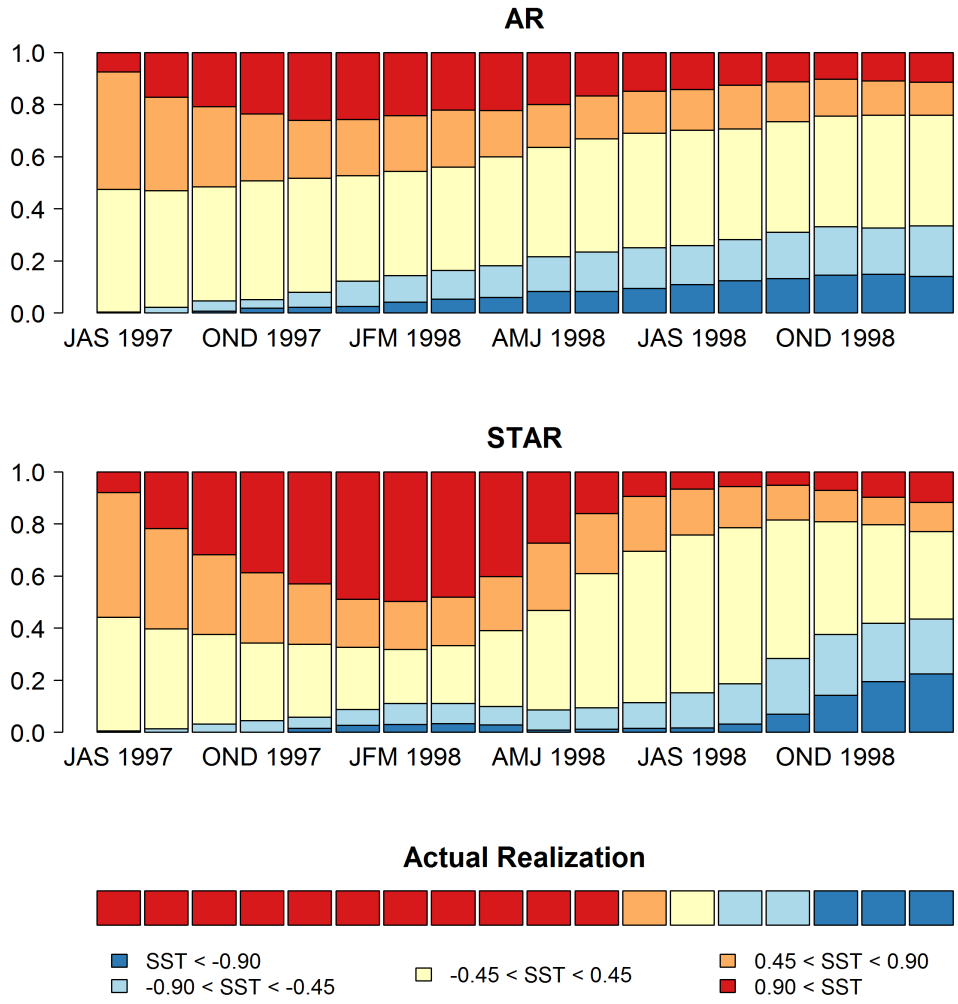

Figure 4: Predicted Cumulative Probabilities of ENSO Several Months Prior to the 1997–1998 El Niño Event

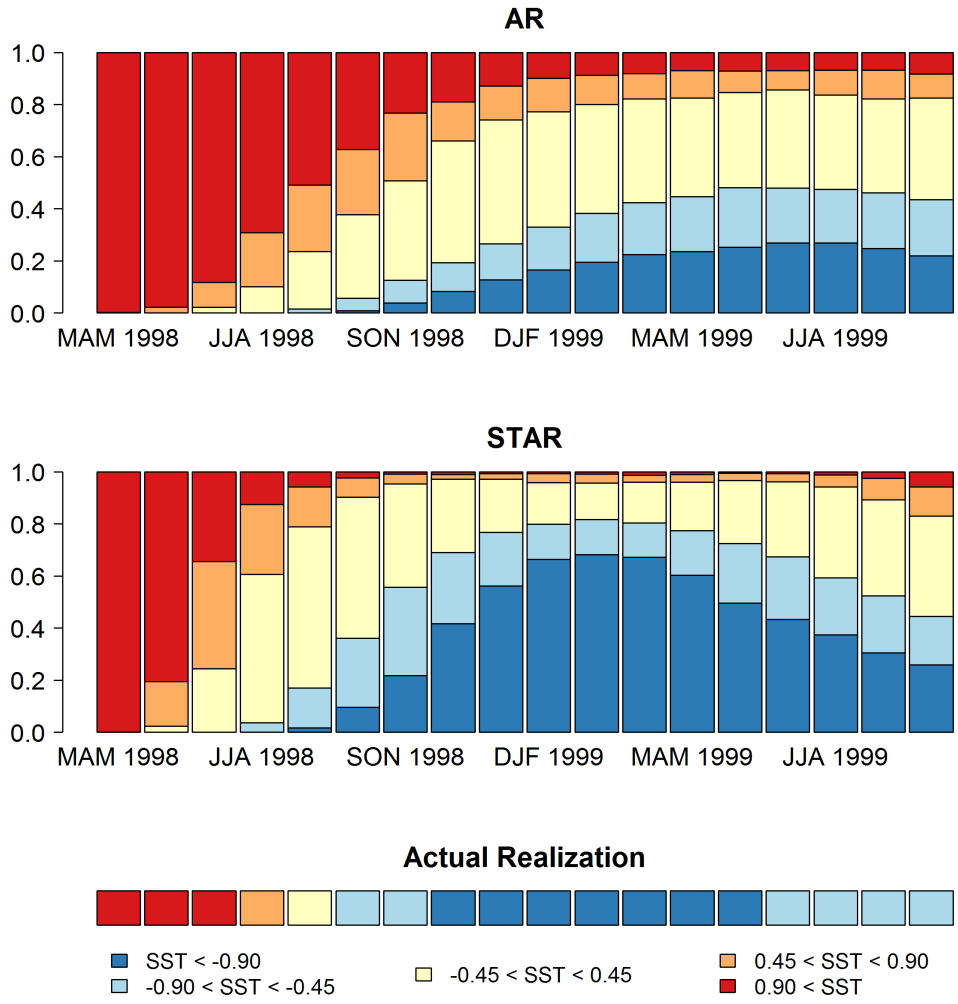

Figure 5: Predicted Cumulative Probabilities of ENSO During the DJF of the 1997–1998 El Niño Event

7 Tables

Table 1: Nonlinearity and Diagnostic Test Results

transition variable, s_t	H_0'	H_{03}	H_{02}	H_{01}
(a) Nonlinearity				
ENSO_{t-1}	4.2e-08	9.5e-01	1.9e-01	3.6e-13
ENSO_{t-2}	7.7e-10	9.9e-01	1.0e-01	1.2e-15
ENSO_{t-3}	2.7e-10	9.8e-01	1.4e-01	3.3e-16
ENSO_{t-4}	1.9e-10	6.3e-01	7.1e-02	2.1e-14
ENSO_{t-5}	6.2e-10	3.5e-01	7.4e-03	2.4e-11
ENSO_{t-6}	2.7e-08	2.1e-01	5.9e-03	1.5e-08
(b) Remaining Nonlinearity and Parameter Constancy				
ENSO_{t-1}	9.3e-01	7.1e-01	8.4e-01	7.9e-01
ENSO_{t-2}	2.6e-01	9.8e-01	2.6e-02	2.7e-01
ENSO_{t-3}	3.7e-01	9.9e-01	1.2e-01	1.4e-01
ENSO_{t-4}	2.6e-01	7.9e-01	6.5e-02	3.5e-01
ENSO_{t-5}	8.8e-02	2.3e-01	1.1e-01	2.8e-01
ENSO_{t-6}	8.0e-02	1.3e-01	1.5e-01	3.1e-01
t^*	2.1e-01	1.6e-01	6.5e-01	1.8e-01

statistics	p-value
(c) Remaining Autocorrelation and Heteroskedasticity	
AC_2	0.011
AC_4	0.053
AC_6	0.137
ARCH_2	0.162
ARCH_4	0.449
ARCH_6	0.350
(d) Residual Normality	
ν	-0.039
κ	3.388
LJB	0.112

Note: The test results are for the window ranging between January 1952 and December 2007. Table entries (except for skewness and kurtosis) are asymptotic probability values of the associated test statistics (as defined in Section 2); ENSO_{t-d}, $d = 1, \ldots, 6$, represents transition variable; $\text{t}^* = t/T$ serves to test for parameter constancy; AC_j and ARCH_j, $j = 2, 4, 6$, represent autocorrelation and autoregressive conditional heteroskedasticity tests of order 2, 4, and 6, respectively; ν abd κ are skewness and kurtosis measures, while LJB is a measure of the Lomnicki-Jarque-Bera test for normality (Lomnicki, 1961; Jarque and Bera, 1987).

Table 2: Parameter Estimates from the Linear AR and Nonlinear STAR Models

	AR		STAR			
	θ		φ_0		φ_1	
variable	estimate	s.e.	estimate	s.e.	estimate	s.e.
intercept	0.000	(0.009)	-0.183	(0.236)	0.282	(0.339)
ENSO_{t-1}	-0.086	(0.012)	-0.116	(0.099)	-0.058	(0.064)
ΔENSO_{t-1}	0.499	(0.038)	0.119	(0.183)	0.455	(0.234)
ΔENSO_{t-2}	-0.086	(0.042)	-0.267	(0.150)	0.268	(0.209)
ΔENSO_{t-3}	0.111	(0.042)	-0.054	(0.129)	0.270	(0.183)
ΔENSO_{t-4}	0.071	(0.042)	-0.065	(0.127)	0.239	(0.187)
ΔENSO_{t-5}	0.059	(0.039)	-0.007	(0.114)	0.122	(0.176)
D_1	0.024	(0.028)	0.114	(0.078)	-0.159	(0.111)
D_2	-0.006	(0.028)	0.354	(0.172)	-0.569	(0.207)
D_3	-0.019	(0.028)	0.340	(0.186)	-0.535	(0.229)
D_4	-0.016	(0.028)	0.177	(0.142)	-0.269	(0.190)
D_5	0.005	(0.028)	0.040	(0.102)	-0.037	(0.154)
D_6	0.045	(0.028)	0.097	(0.100)	-0.078	(0.153)
D_7	0.006	(0.028)	-0.036	(0.098)	0.061	(0.146)
D_8	-0.026	(0.028)	-0.177	(0.116)	0.218	(0.160)
D_9	-0.047	(0.028)	-0.166	(0.098)	0.162	(0.140)
D_{10}	0.044	(0.028)	-0.370	(0.220)	0.651	(0.266)
D_{11}	-0.012	(0.028)	-0.183	(0.100)	0.252	(0.133)

Note: The estimation results are for the window ranging between January 1952 and December 2007. Values in parentheses are asymptotic standard errors of the associated estimates. θ denotes estimates as in Equation (2); φ_0 and φ_1 denote estimates as in Equation (3), so that dynamics of the second regime are to be analyzed by adding up the two parameter vectors.

Table 3: ENSO Forecast Evaluation

h	$\sigma_{\mathrm{l}}/\sigma_{\mathrm{p}}$	$\sigma_{\mathrm{n}}/\sigma_{\mathrm{p}}$	$\sigma_{\mathrm{n}}/\sigma_{\mathrm{l}}$	$\sigma^s_{\mathrm{l}}/\sigma^s_{\mathrm{p}}$	$\sigma^s_{\mathrm{n}}/\sigma^s_{\mathrm{p}}$	$\sigma^s_{\mathrm{n}}/\sigma^s_{\mathrm{l}}$	AR		STAR	
							Niña	*Niño*	*Niña*	*Niño*
1	0.843 **	0.797 **	0.946 **	0.653 **	0.571 **	0.874 **	93.9	90.4	91.8	91.8
2	0.877 **	0.779 **	0.888 **	0.722 **	0.615 **	0.852 **	76.0	74.0	80.0	84.9
3	0.876 **	0.751 **	0.857 **	0.754 **	0.635 **	0.842 **	58.8	56.2	66.7	76.7
4	0.860 **	0.727 **	0.846 **	0.768 **	0.646 **	0.841 **	44.2	47.9	55.8	68.5
5	0.847 **	0.716 **	0.845 **	0.774 **	0.651 **	0.841 **	34.6	38.4	48.1	53.4
6	0.832 **	0.703 **	0.846 **	0.774 **	0.652 **	0.842 **	28.8	26.4	42.3	45.8
7	0.816 **	0.690 **	0.846 **	0.771 **	0.654 **	0.848 **	19.2	16.7	38.5	38.9
8	0.800 **	0.680 **	0.850 **	0.765 **	0.656 **	0.858 **	15.4	8.3	34.6	30.6
9	0.785 **	0.676 **	0.860 **	0.756 **	0.659 **	0.872 **	9.6	5.6	25.0	20.8
10	0.770 **	0.673 **	0.874 **	0.745 **	0.661 **	0.887 **	7.7	2.8	23.1	11.1
11	0.756 **	0.673 **	0.890 **	0.735 **	0.664 **	0.903 **	5.8		23.1	4.2
12	0.744 **	0.674 **	0.906 **	0.726 **	0.666 **	0.917 **	3.8		21.2	
13	0.734 **	0.674 **	0.919 **	0.718 **	0.668 **	0.931 **	1.9		17.3	
14	0.724 **	0.676 **	0.933 **	0.709 **	0.670 **	0.945 **			11.5	
15	0.715 **	0.677 **	0.946 **	0.700 **	0.670 **	0.958 **			13.5	
16	0.708 **	0.679 **	0.959 **	0.689 **	0.669 **	0.970 **			13.5	
17	0.698 **	0.678 **	0.971 **	0.679 **	0.667 **	0.982 **			11.5	
18	0.687 **	0.675 **	0.983 **	0.671 **	0.665 **	0.992			9.6	
19	0.678 **	0.673 **	0.993	0.664 **	0.663 **	0.999			5.8	
20	0.671 **	0.671 **	1.000	0.660 **	0.662 **	1.003			5.7	
21	0.668 **	0.670 **	1.003	0.657 **	0.661 **	1.006				
22	0.665 **	0.669 **	1.006	0.656 **	0.662 **	1.009				
23	0.662 **	0.667 **	1.009	0.657 **	0.665 **	1.012				
24	0.659 **	0.667 **	1.012	0.663 **	0.672 **	1.014				
25	0.659 **	0.669 **	1.014	0.673 **	0.683 **	1.016				
26	0.665 **	0.675 **	1.015	0.686 **	0.698 **	1.017				
27	0.674 **	0.685 **	1.017	0.702 **	0.714 **	1.017				
28	0.687 **	0.699 **	1.017	0.719 **	0.730 **	1.016				
29	0.702 **	0.714 **	1.016	0.736 **	0.746 **	1.014				
30	0.718 **	0.728 **	1.014	0.753 **	0.762 **	1.012				
31	0.736 **	0.744 **	1.012	0.768 **	0.777 **	1.011				
32	0.752 **	0.760 **	1.011	0.782 **	0.789 **	1.009				
33	0.767 **	0.774 **	1.009	0.790 **	0.796 **	1.007				
34	0.782 **	0.788 **	1.007	0.792 **	0.796 **	1.005				
35	0.794 **	0.798 **	1.005							
36	0.795 **	0.797 **	1.002							

Note: entries in the column headed with h denote forecast horizon; σ_{i}, $i = \{p, l, n\}$ represent root mean squared errors from monthly persistence, AR and STAR forecasts, respectively; the similar measures but for the three-month-average SST anomaly are denoted by σ^s_{i}. Further, ** denotes the statistical significance of CW (Clark and West, 2007) measure at 0.05 significance level. Finally, entries in the columns headed with *Niña* and *Niño* denote the percent of correctly predicted measures of each respective ENSO event from the associated (AR or STAR) model.